PCCP

PAPER

View Article Online
View Journal | View Issue

Cite this: *Phys. Chem. Chem. Phys.*, 2016, **18**, 3065

Relationship between vesicle size and steric hindrance influences vesicle rupture on solid supports†

Joshua A. Jackman,[ab] Min Chul Kim,[ab] Vladimir P. Zhdanov[abc] and Nam-Joon Cho*[abd]

Received 6th November 2015,
Accepted 15th December 2015

DOI: 10.1039/c5cp06786c

www.rsc.org/pccp

Phospholipid assemblies on solid supports mimic the cell membrane, and provide a platform to study membrane biology. Among the different types of model membranes, the planar bilayer is a two-dimensional lipid bilayer sheet that can be formed by the adsorption and spontaneous rupture of vesicles. The formation process is influenced by the interactions between vesicles and the solid support as well as between vesicles. On silicon oxide, which is a commonly used solid support, vesicles typically adsorb until reaching a critical coverage and then spontaneous rupture begins. Although it is generally understood that spontaneous rupture leads to planar bilayer formation, oversaturation of vesicles at the critical coverage can hinder the whole process due to a steric factor. To date, the role of this factor has been scrutinized only in relation to temperature, and the influence of additional parameters remains to be elucidated. In this work, we have investigated how vesicle size and corresponding steric constraints influence the kinetics of vesicle adsorption and rupture and, more specifically, how the state of adsorbed vesicles after fusion depends on the vesicle size. Using quartz crystal microbalance-dissipation (QCM-D) and fluorescence recovery after photobleaching (FRAP), we characterized the adsorption kinetics of vesicles onto silicon oxide and the lateral mobility of solid-supported lipid assemblies. While the vesicle adsorption kinetics were diffusion-limited up to the onset of vesicle rupture, the extent of rupture depended on vesicle size and it was observed that larger vesicles are more prone to steric effects than smaller vesicles. We discuss this finding in terms of the structural transformation from adsorbed vesicles to a planar bilayer, including how the interplay of thermodynamic, kinetic and steric factors can affect vesicle rupture on solid supports.

Introduction

Phospholipid assemblies on solid supports represent an important model system to mimic cell membranes, and are widely used in scientific research ranging from fundamental studies on membrane biology to applications such as biosensors and drug development.[1–6] One of the most popular types of model membranes is the planar bilayer, which is a two-dimensional lipid bilayer sheet on a solid support.[1–3,6] The adsorption of lipid vesicles onto a surface followed by rupture is a conventional method to form solid-supported planar bilayers[1,7–9] (for other methods, see, *e.g.*, ref. 10 and references therein). There are several pathways by which vesicle rupture after adsorption may occur, and the relative role of these pathways depends on a multitude of factors including surface composition and topology, vesicle size, lipid composition, solution pH, ionic strength, osmotic pressure, and divalent cations (see ref. 9 and references therein).

Concerning vesicle size, it is thermodynamically favorable for individual vesicles above a certain size to rupture upon adsorption.[11–13] Kinetically, however, the process is subtle. The rate of rupture of vesicles depends on the deformation of their shape during adsorption. In particular, the rupture process is expected to start near the edge of the vesicle–substrate contact area because deformation is at the maximum there[14,15] (for recent complementary and/or alternative viewpoints, see ref. 16 and 17). In general, larger vesicles are expected to be deformed

[a] *School of Materials Science and Engineering, Nanyang Technological University, 50 Nanyang Avenue 639798, Singapore. E-mail: njcho@ntu.edu.sg*
[b] *Centre for Biomimetic Sensor Science, Nanyang Technological University, 50 Nanyang Drive 637553, Singapore*
[c] *Boreskov Institute of Catalysis, Russian Academy of Sciences, Novosibirsk 630090, Russia*
[d] *School of Chemical and Biomedical Engineering, Nanyang Technological University, 62 Nanyang Drive 637459, Singapore*

† Electronic supplementary information (ESI) available: More information is provided about lognormal distribution fit for the DLS data (Fig. S1), kinetic analysis of vesicle adsorption onto silicon oxide (Fig. S2) and the FRAP experiments for lipid assemblies on silicon oxide (Fig. S3). See DOI: 10.1039/c5cp06786c

to a greater extent.[18–20] The vesicle shape near the edge can be characterized by the contact angle which, however, is nearly independent of vesicle size.[13] This means that in this region the substrate-induced vesicle deformation is independent of vesicle size as well. In turn, the latter indicates that the substrate-induced contribution to the activation barrier for rupture is expected to be nearly independent of vesicle size (this is confirmed by 2D Monte Carlo simulations[14]). The membrane curvature of small vesicles is, however, larger, and this may facilitate rupture (the effect of membrane curvature was recently identified in various membrane processes[21–23]). In the case of large vesicles, on the other hand, the length of the edge is longer, and due to this factor the rate of rupture may be higher. Recent simulations by dissipative particle dynamics suggest that small vesicles are in fact more inclined to rupture than larger vesicles.[24] Adding to the complexity of the situation, experimental findings have shown that the interaction of vesicles with a solid support is surface-specific and that vesicle rupture can only occur on a subset of materials, including mica[25,26] and silicon oxide,[7,27] independent of vesicle size.

During adsorption on silicon oxide, zwitterionic lipid vesicles have long been observed by quartz crystal microbalance-dissipation (QCM-D) and related surface-sensitive measurement techniques to remain intact until reaching a critical coverage and then rupture to form a bilayer.[7,28–31] The degree of critical coverage required to commence vesicle rupture is independent of the adsorption rate, suggesting that the interaction between vesicles is necessary to promote rupture on this pathway.[32] In part, this observation can be understood by the fusion of smaller vesicles to form larger vesicles that are more likely to rupture based on thermodynamic arguments presented by Seifert and Lipowsky.[13,33,34] An atomic force microscopy (AFM) study by Reviakine and Brisson supports the mechanism of vesicle fusion prior to rupture by demonstrating that small vesicles fuse to form larger vesicles which can then rupture on mica.[25] The same study also identified the spontaneous rupture of sufficiently large vesicles to form bilayer disks.[25] On mica, the critical radius at which vesicles begin to rupture spontaneously was estimated to be *ca.* 75 nm.[25] By contrast, on glass, small vesicles extruded through 100 nm pores remain intact at low lipid concentration but begin to rupture as the concentration increases.[35] Compared to mica, the critical radius on glass is larger and has been approximated to be greater than 250 nm (up to 2 μm based on calculations).[35] Hence, on multiple silica-based substrates, it has been shown that the interactions between vesicles may promote vesicle fusion events which can form larger vesicles that are more likely to rupture.

Despite these findings, it is still not well understood how vesicle size affects vesicle fusion and rupture, especially when comparing theory and experiment. Reimhult *et al.* have shown that the adsorption kinetics of zwitterionic lipid vesicles onto silicon oxide is qualitatively similar for vesicles with average sizes between 25 and 200 nm in diameter.[36] Specifically, the adsorption of vesicles must reach a critical coverage before rupture can begin. A fluorescence assay that monitored the adsorption of single vesicles onto a quartz substrate also showed a weak dependence of vesicle fusion and rupture on vesicle size.[37] Collectively, these findings underscore the importance of interactions between vesicles because it would be expected that individual, large vesicles rupture immediately upon adsorption if only considering the theory behind the adsorption of single vesicles.[13,33,34] Indeed, based on theory, it would be predicted that vesicles of *ca.* 250 nm radius or greater would rupture immediately upon adsorption onto silicon oxide.[35] However, this has not been observed experimentally. Recently, we also demonstrated that vesicle lamellarity is another important related parameter to control in order to optimize planar lipid bilayer formation.[38] Taken together, these results suggest that other factors are important to explain the behavior of adsorbed vesicles on solid supports.

Additionally, there are other consequences of the interaction between vesicles that need to be considered. By monitoring the formation of a planar bilayer on silicon oxide across the temperature range of 273 K to 303 K, Reimhult *et al.* observed that vesicle rupture is thermally activated.[39,40] In general, the amount of adsorbed vesicles corresponding to the critical coverage at which rupture begins increases at lower temperatures. Based on the surface pinning of adsorbed vesicles,[41] the most likely model to explain spontaneous vesicle rupture after reaching a critical coverage is related to vesicle clustering which arises from the random adsorption of vesicles onto silicon oxide.[42] At low coverage, the adsorption of an additional vesicle does not affect the stress distribution of the already adsorbed vesicles.[14] However, as the coverage of vesicles becomes appreciable, the adsorption of an additional vesicle will generate more stress, thereby lowering the activation barrier. Monte Carlo simulations reported by Dimitrievski *et al.* have been able to reproduce these experimental findings based on the adsorption and surface packing of vesicles.[43]

At the same time, this simple model is not able to describe all cases of spontaneous vesicle rupture after reaching a critical coverage. At sufficiently low temperature, the activation energy is too high for vesicle rupture to occur on silicon oxide, and vesicles adsorb monotonically until forming a close-packed layer.[40] If the temperature is increased during the experiment, then the activation energy may be overcome but vesicle rupture is incomplete.[40] This situation has been attributed to oversaturation of vesicles on the substrate whereby vesicles may actually be sterically stabilized by neighboring vesicles.[40] While steric stabilization has been observed in relation to temperature, it is not well understood if additional experimental parameters may contribute to a steric factor that influences vesicle rupture. Since steric stabilization is related to the surface coverage of vesicles, we surmised that vesicle size may promote steric hindrance. To test this hypothesis, we investigated the effects of vesicle size on the vesicle rupture process on silicon oxide.

Compared to previous works related to the subject,[36,40] we have used a wider size range of vesicles, and characterized both the adsorption kinetics of vesicles onto silicon oxide and the lateral mobility of solid-supported lipid assemblies by employing quartz crystal microbalance-dissipation (QCM-D) and fluorescence recovery after photobleaching (FRAP), respectively. Based

on this combination of measurement techniques, we have scrutinized how the state of zwitterionic lipid vesicles after fusion depends on vesicle size. Using a kinetic model that accounts for the diffusion of vesicles in solution and the critical coverage of vesicles on the solid support, the onset of vesicle rupture is shown to depend linearly on vesicle size in accordance with diffusion-limited kinetics.[32] However, we also identify that larger vesicles are more prone to steric effects that stabilize adsorbed vesicles, thereby hindering the rupture process. Collectively, these findings provide insight into how thermodynamic, kinetic and steric factors affect vesicle rupture on solid supports, particularly in the context of vesicle rupture after reaching a critical coverage.

Materials and methods

Vesicle preparation

Small unilamellar vesicles composed of 1-palmitoyl-2-oleoyl-*sn-glycero*-3-phosphocholine (POPC) (Avanti Polar Lipids, Alabaster, AL) were prepared by the extrusion method, as previously described.[44] The fluorescently labeled lipid, *N*-(7-nitrobenz-2-oxa-1,3-diazol-4-yl)-1,2-dihexadecanoyl-*sn-glycero*-3-phosphoethanolamine (Texas Red-DHPE) (Molecular Probes, Eugene, OR) was added at a molar percentage of 99.5% POPC to 0.5% Texas Red-DHPE for FRAP measurements. After mixing the lipids in chloroform, the solvent was evaporated under nitrogen gas, forming a dried lipid film. After being stored overnight in a vacuum desiccator to remove chloroform, the lipid film was hydrated in water at a nominal lipid concentration of 5 mg mL^{-1}. The suspension was then vortexed for 5 min to form large multilamellar vesicles. Afterwards, the vesicles were passed through track-etched polycarbonate membranes of either 1000, 400, 200, 100, 50 or 30 nm pore sizes a minimum of 19 times by using a miniextruder (Avanti Polar Lipids). The resulting vesicles were diluted to 0.1 mg mL^{-1} before experiment. A Tris buffer (10 mM Tris and 100 mM NaCl, pH 8.0) was used to dilute the vesicle solutions. All buffer solutions were prepared in 18.2 MΩ cm MilliQ-treated water (Millipore, Billerica, MA).

Dynamic light scattering

A 90Plus particle size analyzer (Brookhaven Instruments) with a 658.0 nm monochromatic laser was used to measure the size distribution of vesicle populations after extrusion. In order to minimize the reflection effect, the scattering angle was set at 90°, and the results were collected by digital autocorrelator software. In this work, the intensity-weighted average diameter and fitted lognormal size distribution is reported for the different vesicle samples.

Quartz crystal microbalance-dissipation

A Q-Sense D300 instrument (Q-Sense AB, Gothenburg, Sweden) was used to monitor *in situ* adsorption of vesicles onto silicon oxide, as described elsewhere.[45,46] Briefly, the crystal was initially driven at its resonance frequency, and then the drive circuit was short-circuited. The exponential decay of the crystal oscillation was recorded and analyzed, yielding the changes in frequency and dissipation at 5, 15, 25 and 35 MHz. The measurement data presented herein were recorded at the third overtone (15 MHz) and normalized. The temperature of the measurement cell was 25.0 °C with an in-cell Peltier element to control thermal fluctuations to within 0.5 °C. Measurements were repeated with a deviation of less than 10% in the frequency and energy dissipation shifts.

Fluorescence recovery after photobleaching

Phospholipid assemblies on silicon oxide-coated quartz crystals (Q-Sense) were imaged using an inverted epifluorescence Eclipse TE 2000 microscope (Nikon, Tokyo, Japan) equipped with a 60× oil immersion objective (NA 1.49), and an Andor iXon+ EMCCD camera (Andor Technology, Belfast, Northern Ireland) camera. The samples were illuminated by a TRITC (rhodamine-DHPE) filter set with a mercury lamp (Intensilight C-HGFIE; Nikon Corporation). Bleaching was performed with a 532 nm, 100 mW laser beam ($d \approx 30$ μm). Corresponding image traces of normalized fluorescence intensity were collected across the bleached spots from minus 1 to 60 s in order to monitor the recovery of the fluorescence signal. FRAP analysis was performed to calculate the coefficients of lipid diffusion in lipid assemblies from the temporal fluorescence intensity profiles of selected regions during the measured recovery period. The Hankel method was employed to obtain the diffusion coefficients, as previously described.[47]

Results and discussion

We first monitored the adsorption kinetics of vesicles onto silicon oxide as a function of their size. The frequency and energy dissipation shifts were monitored as functions of time, and reflect changes in the mass and viscoelastic properties of the adlayer, respectively. The average, intensity-weighted effective diameter of the different vesicle populations was 63, 97, 126, 198 or 529 nm, respectively, as measured by dynamic light scattering. The vesicle polydispersity increased as the average vesicle size became larger (Fig. S1, ESI†). QCM-D measurements were performed to monitor the interaction between extruded vesicles and a silicon oxide substrate, as shown in Fig. 1. A baseline signal in buffer solution was first established for ten minutes before adding a solution of lipid vesicles under batch flow conditions.[46] In all cases, a decrease in the frequency signal occurred initially, indicating that vesicles adsorbed onto the substrate. Depending on the vesicle size, there were differences in the adsorption kinetics that are described below.

For vesicles below 130 nm diameter, a critical coverage of adsorbed vesicles was reached within a few minutes and corresponded to frequency shifts of *ca.* −50 Hz. In this size regime, the mass load corresponding to critical coverage increased as a function of vesicle size. After reaching critical coverage, vesicles ruptured quickly and the QCM-D measurement signals stabilized in less than six minutes. The rupture of small vesicles of *ca.* 100 nm diameter or below led to final changes in frequency and energy dissipation of *ca.* −28 Hz and

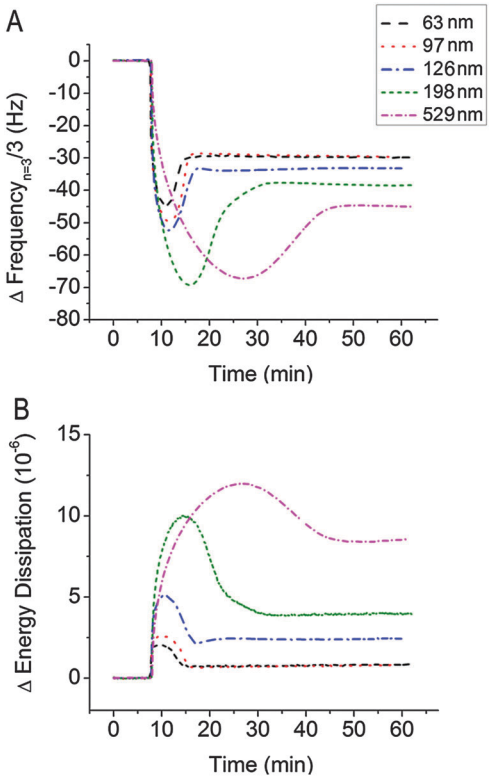

Fig. 1 Influence of vesicle size on vesicle adsorption kinetics. QCM-D monitoring captured the interaction kinetics between lipid vesicles and a silicon oxide support as a function of vesicle size (reported as average diameter). Changes in (A) resonance frequency and (B) energy dissipation, both as functions of time, indicate corresponding changes in mass and viscoelastic properties of the adlayer, respectively.

1×10^{-6}, respectively. These values indicate the formation of a planar bilayer with possibly a small fraction of unruptured vesicles based on the typical frequency and energy dissipation shift values of approximately -26 ± 3 Hz and 1×10^{-6} or less, respectively, for a supported lipid bilayer.[46] The onset of rupture for larger vesicles with 127 nm diameter was kinetically similar, but the rupture process led to final changes in frequency and energy dissipation of *ca.* -35 Hz and 5×10^{-6}, respectively. These values are greater than those corresponding to a planar bilayer, and indicate that rupture is either incomplete or that the lipids form complex aggregates after rupture.

The adsorption of larger vesicles showed kinetic profiles that were similar to the 127 nm diameter case. However, there were also important differences. A critical coverage of adsorbed vesicles was reached more slowly for larger vesicles, taking up to 8 and 20 minutes for vesicles of 198 and 529 nm diameter, respectively. The change in frequency corresponding to the critical coverage was *ca.* -70 Hz in each case with energy dissipation values in the range of 10–12 $\times 10^{-6}$. Hence, in the large vesicle regime, the correlation between the mass load at the critical coverage and vesicle size was no longer valid. After rupturing of vesicles with 198 nm diameter, the final changes in frequency and energy dissipation were -40 Hz and 4×10^{-6}, respectively. The rupture of vesicles with 529 nm diameter led to final changes in frequency and energy dissipation of -50 Hz and 9×10^{-6}, respectively, values which are greater than those of a planar lipid bilayer.

Interestingly, previous findings by Reimhult *et al.* support that vesicles rupture to form a planar bilayer independent of vesicle size (up to 200 nm average diameter), albeit the kinetics of the process depend on vesicle size.[36,40] To reconcile this difference between the two studies, it is noteworthy that a different extrusion filter was used in the present study, as compared to the former.[48] Using our extrusion apparatus, we have previously reported that large extruded vesicles typically exhibit a polydisperse size distribution.[22,49] The fraction of large-size vesicles can impair bilayer formation, even after extensive freeze–thaw pretreatment.[49] Furthermore, in the former studies,[36,40] the external ionic strength was 150 mM NaCl whereas it was 100 mM NaCl in the present study. Based on extended-DLVO model calculations,[9] it has been recently shown that, near the substrate, the vesicle–silicon oxide interaction energy can be significantly affected by subtle differences in the ionic strength within this range. Hence, the rupture process may be mediated in part by the strength of the vesicle–substrate interaction with the relative contribution of steric hindrance depending on vesicle size.

Based on these observations, we draw attention to particular aspects of the adsorption and rupture of vesicles on silicon oxide for further scrutiny. Upon reaching the critical coverage, small vesicles rupture to form a nearly complete planar bilayer. Large vesicles also rupture at this point, but do not form a complete planar bilayer. It is unknown whether the rupture of larger vesicles is incomplete or the lipids form complex aggregates after rupture. We address this question by analyzing the changes in structural properties of the lipid assembly during the adsorption and rupture process, as monitored in the QCM-D experiments. To remove the dependence on time, we plotted time-independent curves that describe the relationship between changes in frequency and energy dissipation during the adsorption and rupture process (Fig. 2).

For vesicles populations with diameters smaller than 200 nm, the curves show two stages corresponding to before and after vesicle rupture, respectively. The differences between these two stages indicate that the rupture process causes the release of energy-dissipating materials. For a given value of the change in frequency, the related change in energy dissipation signal has a greater value in the stage before rupture *versus* the stage after rupture. The slopes increase as a function of vesicle size, which is reasonable because larger vesicles have a greater mass fraction from hydrodynamically-coupled solvent. As a result, the adsorption of larger vesicles causes a greater change in energy dissipation per change in frequency due to the increased solvent-to-lipid ratio. Based on these plots, the properties of the resulting lipid assemblies can be interpreted. For vesicles between 120 and 200 nm diameter, the lipid assemblies have viscoelastic properties that do not reflect the properties of a planar bilayer. By contrast, for vesicles below 100 nm diameter, the plots converge, indicating the formation of a nearly complete bilayer.

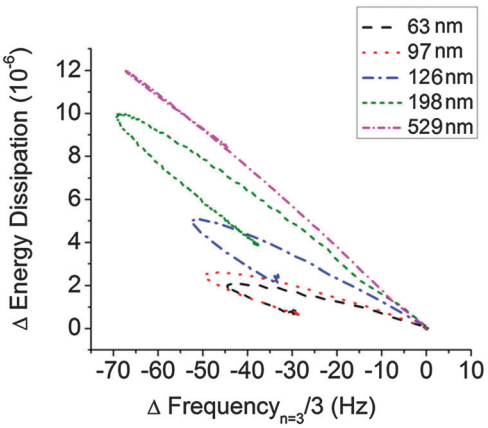

Fig. 2 Structural transformation of adsorbed vesicles on silicon oxide. Based on the QCM-D plots in Fig. 1, time-independent curves describe the relationship between changes in resonance frequency and energy dissipation as a function of vesicle size (reported as average diameter). For smaller vesicles, a structural transformation from intact vesicles to planar lipid bilayer is observed. For larger vesicles, no such transformation is observed despite evidence of vesicle rupturing.

A considerably different adsorption profile was also observed for vesicles with 529 nm diameter. In this case, there was a linear correspondence between changes in frequency and energy dissipation. This feature is surprising because the QCM-D adsorption kinetics indicate that there is mass loss after the critical coverage was reached. That is, a critical coverage corresponding to the onset of spontaneous vesicle rupture was observed but it is unlikely the physical properties of the adsorbate—that is, the adsorbed vesicles—change during the adsorption process. This case is possible in the event that only a few vesicles ruptured while the overall physical properties of the adlayer did not change—*i.e.*, most adsorbed vesicles remained intact with encapsulated, hydrodynamically-coupled solvent. Several lines of evidence support this statement. First, there is no cusp in the curve that would indicate the rupture of vesicles globally across the entire surface. If all or a majority of the vesicles actually did rupture and the lipids formed complex aggregates thereafter, a change in the physical properties of the film would be expected but this did not occur. In addition, the curve for the adsorption profile in this case shows the same behavior as that observed for a layer of adsorbed, intact vesicles.[40] The similarity between the two cases further supports that a structural transformation does not occur within the adsorbed film, and that the adlayer retains the bulk properties of a layer of intact vesicles.

To summarize, three types of adsorption profiles are observed for the vesicle-to-bilayer structural transformation based on time-independent plot analysis. For small vesicles, the profile indicates the process of vesicle rupture leading to the formation of a nearly complete bilayer. For vesicles of intermediate size, the profile also indicates the same process of vesicle rupture but the resulting changes in resonance frequency and energy dissipation do not compare well with that of a complete bilayer. For the largest size vesicles in this study, the profile indicates there is no change in the physical properties of the adsorbate. More comprehensively, these findings suggest that deviations in the mass and viscoelastic properties of a lipid assembly, as compared to the properties of a complete bilayer, are due to unruptured vesicles rather than lipids forming complex aggregates. Based on the observed effects of vesicle size on bilayer formation, the adsorption profiles also do not agree with thermodynamic arguments supporting the preferred rupture of individual vesicles with sizes larger than the critical one. Hence, other factors are likely important to explain the dependence of the vesicle adsorption kinetics on vesicle size.

Kinetic aspects

To understand the effects of vesicle size on the vesicle adsorption profile, we constructed a kinetic model that accounts for the diffusion of lipid vesicles in solution and the critical coverage of vesicles on the solid support (Fig. 3). In this model, until reaching the critical coverage, the rupture of adsorbed vesicles is assumed to be negligible. This assumption is supported by control experiments that show interruption of vesicle adsorption at or before the critical coverage abrogates vesicle rupturing.[32,36] For this reason, the stage can be described in the model by taking only vesicle adsorption into account. Vesicles are relatively large, and their adsorption is controlled by diffusion almost up to saturation.[50] Under the batch flow conditions of the experiment, the diffusion flux per unit support area is defined as[51]

$$J = \left(\frac{D}{\pi t}\right)^{1/2} c \qquad (1)$$

where D is the diffusion coefficient ($cm^2\ s^{-1}$), and c is the vesicle concentration (cm^{-3}) in solution. This expression can also be represented as

$$J = Dc/\delta \qquad (2)$$

where $\delta = (\pi Dt)^{1/2}$ is the corresponding diffusion length. The surface concentration (cm^{-2}) of vesicles is accordingly given by

$$C = 2\pi^{-1/2}(Dt)^{1/2}c \qquad (3)$$

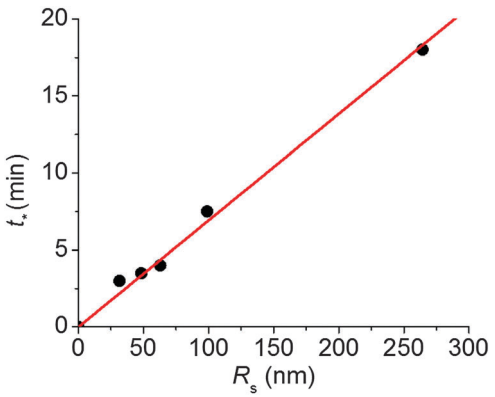

Fig. 3 Relationship between vesicle size and rupturing kinetics. Based on the QCM-D resonance frequency data (Fig. 1A), the time at which vesicle rupturing commences is plotted as a function of vesicle size. A linear dependence is observed, demonstrating that vesicle rupture follows diffusion-limited kinetics with the critical coverage nearly independent of vesicle size.

while the surface coverage is

$$\theta \equiv \pi {R_a}^2 C = 2\pi^{1/2} {R_a}^2 (Dt)^{1/2} c \quad (4)$$

where R_a is the radius of the area occupied by an adsorbed vesicle. According to hydrodynamics, the vesicle diffusion coefficient figuring in these equations is represented as

$$D = \frac{k_B T}{6\pi\eta R_s} \quad (5)$$

where R_s is the average vesicle radius in solution, and η is the viscosity. If θ_* is the critical coverage, then the corresponding time t_* can be estimated by using eqn (4). Under the experimental conditions, the mass concentration of lipid in solution is constant. This means that $c \propto 1/{R_s}^2$. With this relation and eqn (5), eqn (4) yields

$$t_* \propto \theta_*^2 {R_s}^5 / {R_a}^4 \quad (6)$$

The simplest scenario might be that $R_a \cong R_s$, or that the shape of vesicles of different size is self-similar, *i.e.*, $R_a \propto R_s$, and the critical coverage is independent of vesicle size. In this case, eqn (6) yields

$$t_* \propto R_s \quad (7)$$

Overall, the experimental results agree well with the model and reflect the dependence of t_* on R_s (see Fig. 3). We also replotted past experimental results from Reimhult *et al.*[36] and confirmed this relationship (data not shown).

As already noted, the experiments indicate that vesicle rupture occurs after reaching a critical coverage of adsorbed vesicles on silicon oxide. Mechanistically, this means that the rupture process is related to the interactions between vesicles. From this perspective, the approximately linear dependence of t_* on R_s indicates that interactions between vesicles are equally favorable nearly independent of vesicle size.

Although the deviation is minor, it is also noteworthy that, in the small vesicle regime (diameter below 130 nm), the rupture behavior therein can be described more accurately by $t_* \propto {R_s}^{1/2}$ (Fig. S2, ESI†). A weaker dependence of t_* on R_s can be explained by the shape of vesicles not being self-similar in this regime (see, *e.g.*, Monte Carlo simulations[19]). Concomitantly, the ratio R_a/R_s can increase rather significantly with increasing R_s in this regime. According to eqn (6), this will result in a weaker dependence of t_* on R_s compared to (7). Alternatively, the contrast ratio remains fairly uniform for larger vesicles, which does not allow us to scrutinize the situation in more detail by using eqn (6). Nevertheless, the rupture kinetics of larger vesicles must be considered alongside steric effects that may affect the outcome of the vesicle-to-bilayer structural transformation.

Based on the proposed model that larger, adsorbed vesicles are less likely to rupture due to steric effects, we also performed FRAP measurements on lipid assemblies (complete or incomplete supported lipid bilayers) in order determine how unruptured vesicles would affect the fluidic properties of supported membranes (Table 1 and Fig. 4; see also Fig. S3, ESI†). After the rupture of small vesicles (50–75 nm diameter), the diffusion coefficient of a fluorescently labeled lipid within the resulting lipid layer was approximately 2 $\mu m^2\ s^{-1}$. This value matches reported values of a planar bilayer on silicon oxide.[52] The rupture of intermediate-size vesicles (between 100–170 nm diameter) formed lipid layers with a diffusion coefficient of 1.5 $\mu m^2\ s^{-1}$, which is also within the range for a relatively complete planar bilayer. By contrast, the rupture of larger vesicles (190 nm or greater diameter) resulted in lipid layers with diffusion coefficients of 0.9 $\mu m^2\ s^{-1}$, respectively. Moreover, there was a decrease in the mobile fraction of lipids in the fabricated supported lipid bilayers from 96.8 ± 2.7% (smallest vesicle case) to 54.8 ± 1.3% (largest vesicle case). Taken together, the trends in diffusion coefficient and mobile fraction are consistent with larger vesicles being less prone to rupture.

Table 1 Lateral diffusion of phospholipid assemblies on silicon oxide. FRAP experiments were performed on phospholipid assemblies after the rupture of vesicles on silicon oxide. The mobility of phospholipids was determined by calculating the diffusion coefficient, and the percent recovery of fluorescence in the bleached spot was also estimated

Vesicle diameter (nm)	Mobility ($\mu m^2\ s^{-1}$)	Recovery (%)
57	2.11 ± 0.10	96.8 ± 2.7
75	1.92 ± 0.11	87.2 ± 0.5
97	1.56 ± 0.01	81.2 ± 1.6
174	1.54 ± 0.03	80.0 ± 0.9
192	0.90 ± 0.13	71.7 ± 3.4
339	0.86 ± 0.03	54.8 ± 1.3

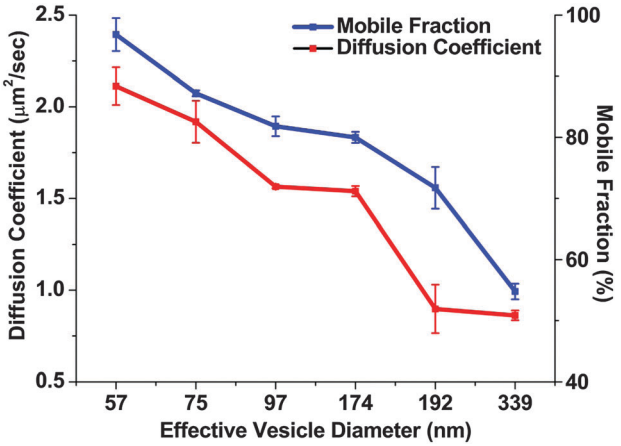

Fig. 4 Trends in lipid mobility as a function of vesicle size. The diffusion coefficient and mobile fraction are presented as a function of vesicle size corresponding to average vesicle diameter.

Fluorescence microscopy experiments further support this proposed model by offering direct experimental evidence that the number density of unruptured vesicles in a supported lipid bilayer increases with larger average vesicle sizes.[53] In terms of the effects on membrane fluidity, the unruptured vesicles have significant detrimental effects by acting as obstacles that impede the diffusion path of lipids in the contiguous planar lipid bilayer.[54] Indeed, Jung *et al.* reported similar effects of nm-scale, polymerized bilayer pattern fragments on the diffusion properties of otherwise fluidic planar bilayers.[55] The steric

effects contributing to inefficient bilayer formation from large vesicles also translate into mobility drawbacks which relate to the presence of unruptured vesicles as diffusion barriers. Hence, there is a correlation between the adsorption kinetics of vesicles onto silicon oxide and the resulting physical properties of the lipid assemblies, with the common parameter being vesicle size. Collectively, the experimental findings support that large vesicles do not rupture due to steric hindrance and, consequently, the unruptured vesicles act as diffusion barriers that hinder lateral diffusion.

As discussed above, our experiments indicate that vesicles adsorb onto silicon oxide until reaching a critical coverage and then rupture. In this pathway, the rate-limiting step is understood to be vesicle rupture. Therefore, it is seemingly counterintuitive that the kinetics of vesicle adsorption are approximately diffusion-limited up to the onset of rupture irrespective of vesicle size, yet the outcome of the rupture process varies depending on the vesicle size. In particular, after the critical coverage is reached and rupture begins, the physical properties of the adlayer of large vesicles remain similar to those of intact vesicles, while the properties of the adlayer of small vesicles change appreciably. One possible explanation is related to the mass load corresponding to the critical coverage at which rupture begins, namely that a greater mass load promotes steric hindrance.

As already noticed in the Introduction, past studies on the temperature-dependence of vesicle rupture on silicon oxide provide a model to understand steric effect.[39,40] Since the rupture of vesicles on silicon oxide is thermally activated, more interactions between vesicles are needed to initiate rupture at lower temperature.[39,40] As a result, a higher mass load is required at lower temperature in order to initiate vesicle rupture at the critical coverage. However, there is also another effect. The higher mass load of adsorbed vesicles can promote steric effects between adsorbed vesicles. When vesicles begin to rupture at lower temperature, a complete bilayer does not form. Rather, the formation of ''patchy'' bilayers consisting of both bilayer fragments and unruptured vesicles has been observed.[43] To explain this behavior, Reimhult, Höök and Kasemo have argued that steric hindrance may be caused by oversaturation of vesicles on the surface and can actually stabilize adsorbed vesicles rather than promote rupture.[40]

In relation to steric stabilization, another potential factor to consider is vesicle lamellarity. The extrusion process typically reduces lamellarity to form unilamellar vesicles, and this effect is most pronounced when vesicles are extruded through small pores[56] (especially 100 nm diameter or smaller pores[57]). Hence, it is possible that the observed adsorption kinetics of larger vesicles are due in part to the presence of some multilamellar vesicles remaining. However, lamellarity alone cannot explain our findings as evidenced by our recent observations that the quality of planar bilayers formed from freeze–thaw pretreated vesicles is still significantly affected by vesicle size.[49] Taken together, the findings demonstrate there is a relationship between vesicle size and steric hindrance that can influence vesicle rupture on solid supports depending on the system specifics (*e.g.*, vesicle–substrate interaction). In terms of practical application, this means that for the pathway whereby vesicles adsorb until reaching a critical coverage, smaller vesicles promote more complete rupture presumably due to the absence of steric constraints and hence are more useful for formation of planar bilayers on solid supports.

Conclusion

In this work, we have investigated the effect of vesicle size on the interaction between vesicles and silicon oxide. Across a wide range of vesicle sizes, the adsorption of intact vesicles onto silicon oxide was observed until reaching a critical coverage and then rupture of vesicles began. QCM-D monitoring indicated that the rupture of small vesicles formed relatively complete bilayers, and the rupture of large vesicles was incomplete and resulted in a mixed layer of bilayer and intact vesicles. The corresponding kinetics were described by using a model which implies that vesicle adsorption is limited by diffusion in solution and the rupture begins at a time that is approximately proportional to vesicle size. One of the interpretations of these findings is that the critical coverage at which rupture commences is nearly independent of vesicle size. However, larger vesicles are also subject to steric effects that prevent rupture of at least some of them. FRAP experiments indicate that intact vesicles act as diffusion barriers that hinder the lateral lipid diffusion of lipid assemblies adsorbed on the substrate after vesicle rupture. Taken together, these findings confirm that the rupture of smaller vesicles is preferred to form complete bilayers, help to reconcile theory and experiment, and offer additional insight into the relationship between the kinetics and thermodynamics of vesicle adhesion to solid supports, including the formation of planar bilayers on silicon oxide.

Acknowledgements

The authors wish to acknowledge support from the National Research Foundation (NRF-NRFF2011-01 and NRF2015NRF-POC0001-19) and Nanyang Technological University to N. J. C. V. P. Zh. is a recipient of the Tan Chin Tuan Exchange Fellowship at Nanyang Technological University.

References

1 R. P. Richter, R. Bérat and A. R. Brisson, *Langmuir*, 2006, **22**, 3497–3505.
2 G. J. Hardy, R. Nayak and S. Zauscher, *Curr. Opin. Colloid Interface Sci.*, 2013, **18**, 448–458.
3 A. Mashaghi, S. Mashaghi, I. Reviakine, R. M. Heeren, V. Sandoghdar and M. Bonn, *Chem. Soc. Rev.*, 2014, **43**, 887–900.
4 A. Alessandrini and P. Facci, *Soft Matter*, 2014, **10**, 7145–7164.
5 A. Gunnarsson, A. Snijder, J. Hicks, J. Gunnarsson, F. Höök and S. Geschwindner, *Anal. Chem.*, 2015, **87**, 4100–4103.
6 J. A. Jackman and N.-J. Cho, *Biointerphases*, 2012, **7**, 18.

7 C. Keller and B. Kasemo, *Biophys. J.*, 1998, **75**, 1397–1402.
8 K. Morigaki and K. Tawa, *Biophys. J.*, 2006, **91**, 1380–1387.
9 J. A. Jackman, J. H. Choi, V. P. Zhdanov and N.-J. Cho, *Langmuir*, 2013, **29**, 11375–11384.
10 S. R. Tabaei, J.-H. Choi, G. Haw Zan, V. P. Zhdanov and N.-J. Cho, *Langmuir*, 2014, **30**, 10363–10373.
11 H. Egawa and K. Furusawa, *Langmuir*, 1999, **15**, 1660–1666.
12 A. S. Muresan and K. Y. C. Lee, *J. Phys. Chem. B*, 2001, **105**, 852–855.
13 U. Seifert and R. Lipowsky, *Phys. Rev. A: At., Mol., Opt. Phys.*, 1990, **42**, 4768.
14 V. Zhdanov and B. Kasemo, *Langmuir*, 2001, **17**, 3518–3521.
15 V. P. Zhdanov, *Chem. Phys. Lett.*, 2015, **641**, 20–22.
16 A. r. Takáts-Nyeste and I. Derényi, *Langmuir*, 2014, **30**, 15261–15265.
17 C. Kataoka-Hamai and T. Yamazaki, *Langmuir*, 2015, **31**, 1312–1319.
18 I. Reviakine, F. F. Rossetti, A. N. Morozov and M. Textor, *J. Chem. Phys.*, 2005, **122**, 204711.
19 K. Dimitrievski, *Langmuir*, 2010, **26**, 3008–3011.
20 I. Reviakine, M. Gallego, D. Johannsmann and E. Tellechea, *J. Chem. Phys.*, 2012, **136**, 084702.
21 N. S. Hatzakis, V. K. Bhatia, J. Larsen, K. L. Madsen, P.-Y. Bolinger, A. H. Kunding, J. Castillo, U. Gether, P. Hedegård and D. Stamou, *Nat. Chem. Biol.*, 2009, **5**, 835–841.
22 J. A. Jackman, G. H. Zan, V. P. Zhdanov and N.-J. Cho, *J. Phys. Chem. B*, 2013, **117**, 16117–16128.
23 M. Rabe, S. R. Tabaei, H. Zetterberg, V. P. Zhdanov and F. Höök, *Angew. Chem., Int. Ed.*, 2015, **54**, 1022–1026.
24 H.-L. Wu, P.-Y. Chen, C.-L. Chi, H.-K. Tsao and Y.-J. Sheng, *Soft Matter*, 2013, **9**, 1908–1919.
25 I. Reviakine and A. Brisson, *Langmuir*, 2000, **16**, 1806–1815.
26 L. Boni, S. Minchey, W. Perkins, P. Ahl, J. Slater, M. Tate, S. Gruner and A. Janoff, *Biochim. Biophys. Acta, Biomembr.*, 1993, **1146**, 247–257.
27 A. A. Brian and H. M. McConnell, *Proc. Natl. Acad. Sci. U. S. A.*, 1984, **81**, 6159–6163.
28 T. H. Anderson, Y. Min, K. L. Weirich, H. Zeng, D. Fygenson and J. N. Israelachvili, *Langmuir*, 2009, **25**, 6997–7005.
29 R. Richter, A. Mukhopadhyay and A. Brisson, *Biophys. J.*, 2003, **85**, 3035–3047.
30 E. Reimhult, C. Larsson, B. Kasemo and F. Höök, *Anal. Chem.*, 2004, **76**, 7211–7220.
31 E. Reimhult, M. Zäch, F. Höök and B. Kasemo, *Langmuir*, 2006, **22**, 3313–3319.
32 C. Keller, K. Glasmästar, V. Zhdanov and B. Kasemo, *Phys. Rev. Lett.*, 2000, **84**, 5443–5446.
33 R. Lipowsky and U. Seifert, *Mol. Cryst. Liq. Cryst.*, 1991, **202**, 17–25.
34 U. Seifert, *Adv. Phys.*, 1997, **46**, 13–137.
35 H. Schönherr, J. M. Johnson, P. Lenz, C. W. Frank and S. G. Boxer, *Langmuir*, 2004, **20**, 11600–11606.
36 E. Reimhult, F. Hook and B. Kasemo, *J. Chem. Phys.*, 2002, **117**, 7401–7404.
37 J. M. Johnson, T. Ha, S. Chu and S. G. Boxer, *Biophys. J.*, 2002, **83**, 3371–3379.
38 J. A. Jackman, Z. Zhao, V. P. Zhdanov, C. W. Frank and N.-J. Cho, *Langmuir*, 2014, **30**, 2152–2160.
39 E. Reimhult, F. Höök and B. Kasemo, *Phys. Rev. E: Stat., Nonlinear, Soft Matter Phys.*, 2002, **66**, 051905.
40 E. Reimhult, F. Höök and B. Kasemo, *Langmuir*, 2003, **19**, 1681–1691.
41 S. Klacar, K. Dimitrievski and B. Kasemo, *J. Phys. Chem. B*, 2009, **113**, 5681–5685.
42 V. Zhdanov, C. Keller, K. Glasmästar and B. Kasemo, *J. Chem. Phys.*, 2000, **112**, 900.
43 K. Dimitrievski, E. Reimhult, B. Kasemo and V. P. Zhdanov, *Colloids Surf., B*, 2004, **39**, 77–86.
44 R. C. MacDonald, R. I. MacDonald, B. P. M. Menco, K. Takeshita, N. K. Subbarao and L.-r. Hu, *Biochim. Biophys. Acta, Biomembr.*, 1991, **1061**, 297–303.
45 N.-J. Cho, K. K. Kanazawa, J. S. Glenn and C. W. Frank, *Anal. Chem.*, 2007, **79**, 7027–7035.
46 N.-J. Cho, C. W. Frank, B. Kasemo and F. Höök, *Nat. Protoc.*, 2010, **5**, 1096–1106.
47 P. Jönsson, M. P. Jonsson, J. O. Tegenfeldt and F. Höök, *Biophys. J.*, 2008, **95**, 5334–5348.
48 N. Berger, A. Sachse, J. Bender, R. Schubert and M. Brandl, *Int. J. Pharm.*, 2001, **223**, 55–68.
49 J. A. Jackman, Z. Zhao, V. P. Zhdanov, C. W. Frank and N.-J. Cho, *Langmuir*, 2014, **30**, 2152–2160.
50 T. Zhu, Z. Jiang and Y. Ma, *Colloids Surf., B*, 2012, **97**, 155–161.
51 V. Zhdanov and B. Kasemo, *Proteins: Struct., Funct., Bioinf.*, 1998, **30**, 177–182.
52 C. Hamai, P. S. Cremer and S. M. Musser, *Biophys. J.*, 2007, **92**, 1988–1999.
53 M. C. Kim, A. Gunnarsson, S. R. Tabaei, F. Höök and N.-J. Cho, *Phys. Chem. Chem. Phys.*, 2015, DOI: 10.1039/C5CP06472D.
54 P. Nollert, H. Kiefer and F. Jähnig, *Biophys. J.*, 1995, **69**, 1447–1455.
55 M. Jung, N. Vogel and I. Köper, *Langmuir*, 2011, **27**, 7008–7015.
56 H. Jousma, H. Talsma, F. Spies, J. Joosten, H. Junginger and D. Crommelin, *Int. J. Pharm.*, 1987, **35**, 263–274.
57 L. Mayer, M. Hope and P. Cullis, *Biochim. Biophys. Acta, Biomembr.*, 1986, **858**, 161–168.

